Role of LCN2 in a murine model of hindlimb ischemia and in peripheral artery disease patients, and its potential regulation by miR-138-5P

Saenz-Pipaon, G.; Jover, E.; Bent, M.L. van der; Orbe, J.; Rodriguez, J.A.; Fernández-Celis, A.; ... ; Roncal, C.

Atherosclerosis 385 (2023) 117343

Contents lists available at ScienceDirect

Atherosclerosis

journal homepage: www.elsevier.com/locate/atherosclerosis

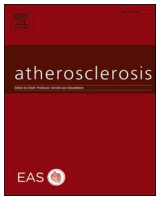

Role of LCN2 in a murine model of hindlimb ischemia and in peripheral artery disease patients, and its potential regulation by miR-138-5P

Goren Saenz-Pipaon [a,b], Eva Jover [b,c], M. Leontien van der Bent [d,e], Josune Orbe [a,b,f], Jose A. Rodriguez [a,b,g], Amaya Fernández-Celis [b,c], Paul H.A. Quax [d,e], Jose A. Paramo [a,b,g,h], Natalia López-Andrés [b,c], Jose Luis Martín-Ventura [g,i], Anne Yaël Nossent [d,e], Carmen Roncal [a,b,g,*]

[a] Laboratory of Atherothrombosis, Cima Universidad de Navarra, Pamplona, Spain
[b] IdiSNA, Instituto de Investigación Sanitaria de Navarra, Pamplona, Spain
[c] Cardiovascular Translational Research, Navarrabiomed (Miguel Servet Foundation), Hospital Universitario de Navarra (HUN), Universidad Pública de Navarra (UPNA), Pamplona, Spain
[d] Department of Vascular Surgery, Leiden University Medical Center, Leiden, the Netherlands
[e] Einthoven Laboratory for Experimental Vascular Medicine, Leiden University Medical Center, Leiden, the Netherlands
[f] RICORS-ICTUS, ISCIII, Madrid, Spain
[g] CIBERCV, ISCIII, Madrid, Spain
[h] Hematology Service, Clínica Universidad de Navarra, Pamplona, Spain
[i] IIS-Fundación Jiménez Díaz, Madrid, Spain

ARTICLE INFO

Keywords:
Inflammation
Atherosclerosis
Vascular disease
Muscle damage
microRNA

ABSTRACT

Background and aims: Peripheral arterial disease (PAD) is a leading cause of morbimortality worldwide. Lipocalin-2 (LCN2) has been associated with higher risk of amputation or mortality in PAD and might be involved in muscle regeneration. Our aim is to unravel the role of LCN2 in skeletal muscle repair and PAD.
Methods and results: WT and *Lcn2*$^{-/-}$ mice underwent hindlimb ischemia. Blood and crural muscles were analyzed at the inflammatory and regenerative phases. At day 2, *Lcn2*$^{-/-}$ male mice, but not females, showed increased blood and soleus muscle neutrophils, and elevated circulating pro-inflammatory monocytes ($p < 0.05$), while locally, total infiltrating macrophages were reduced ($p < 0.05$). Moreover, *Lcn2*$^{-/-}$ soleus displayed an elevation of *Cxcl1* ($p < 0.001$), and *Cxcr2* ($p < 0.01$ in males), and a decrease in *Ccl5* ($p < 0.05$). At day 15, Lcn2 deficiency delayed muscle recovery, with higher density of regenerating myocytes ($p < 0.04$) and arterioles (αSMA^{+}, $p < 0.025$). Reverse target prediction analysis identified miR-138-5p as a potential regulator of LCN2, showing an inverse correlation with *Lcn2* mRNA in skeletal muscles (rho = -0.58, $p < 0.01$). *In vitro*, miR-138-5p mimic reduced *Lcn2* expression and luciferase activity in murine macrophages ($p < 0.05$). Finally, in human serum miR-138-5p was inversely correlated with LCN2 ($p \leq 0.001$ adjusted, n = 318), and associated with PAD (Odds ratio 0.634, $p = 0.02$, adjusted, PAD n = 264, control n = 54).
Conclusions: This study suggests a possible dual role of LCN2 in acute and chronic conditions, with a probable role in restraining inflammation early after skeletal muscle ischemia, while being associated with vascular damage in PAD, and identifies miR-138-5p as one potential post-transcriptional regulator of LCN2.

1. Introduction

Lower limb peripheral artery disease (PAD) is a major cause of atherosclerotic vascular morbidity and mortality worldwide [1]. Importantly, its prevalence is predicted to increase with the aging of the population and the growing incidence of cardiovascular risk factors, representing a serious health economic cost in the future [2]. Lower limb symptoms, e.g.: claudication, are frequent in PAD subjects and are associated with reduced exercise capability, worsened quality of life and increased mortality [3]. Skeletal muscle hypoperfusion, due to the progressive narrowing of the lower limb arteries, is a primary factor leading to muscle degeneration and to claudication symptoms, which

* Corresponding author. Laboratory of Atherothrombosis, Cima Universidad de Navarra, Avda. Pio XII, 55, 31008, Pamplona, Spain.
E-mail address: croncalm@unav.es (C. Roncal).

https://doi.org/10.1016/j.atherosclerosis.2023.117343
Received 28 November 2022; Received in revised form 7 August 2023; Accepted 10 October 2023
Available online 11 October 2023

are aggravated as the disease advances [4]. As such, the identification of new molecules involved in muscle response to ischemia may allow the development of therapies that improve limb-related symptoms in PAD.

By the transcriptomic analysis of circulating extracellular vesicles, our group identified lipocalin-2 (LCN2 or neutrophil-gelatinase associated lipocalin, NGAL) as differentially expressed in critical limb ischemia patients compared to healthy subjects [5], and reported an association between elevated serum LCN2 levels and higher risk of limb amputation or cardiovascular mortality in PAD subjects [6]. LCN2 is a small secreted glycoprotein of the lipocalin family [7] that has been involved in atherosclerosis [8,9]. As such, it was colocalized with matrix metalloproteinase 9 (MMP-9) in human and murine atherosclerotic lesions, and increased LCN2 levels were associated with plaque instability and higher MMP-9 activity in human carotid atheroma [10,11]. LCN2 has also been involved in skeletal muscle repair and extracellular matrix (ECM) remodeling [12]. For instance, in a toxin-induced muscle injury model, LCN2 deficiency attenuated satellite cells (SCs) activation, increased muscle fibrosis and reduced MMP-9 activity [13]. Moreover, LCN2 has been implicated in the modulation of the immune cell response in several *in vivo* and *in vitro* studies with opposing results [9,14].

In this study, we sought to determine the role of LCN2 in skeletal muscle response to ischemia and to study its posttranscriptional regulatory mechanisms. To address our objectives, we subjected wild type (WT) and *Lcn2*$^{-/-}$ mice to femoral artery ligation and analyzed cellular and molecular responses at the degenerative phase of muscle repair (day 2), and morphological changes at the regenerative phase (day 15) [15]. Moreover, we applied an *in silico* approach to identify possible post-transcriptional regulators of LCN2, focusing on micro-RNAs (miRNAs). Finally, we determined the relationship between LCN2 and one of its potential posttranscriptional regulators, miR-138-5p, in blood of PAD and control subjects.

2. Materials and methods

A complete description of material and methods is available in the Supplemental information file.

2.1. Hindlimb ischemia (HLI) model

Wild type (WT, C57Bl/6J, Envigo) and *Lcn2* deficient (Lcn2^{tm1Mak}, C57Bl/6J background) [16] 12-week-old male and female mice (n = 20–26 mice per genotype per sex) were anesthetized with isoflurane (2.5%–4%, inhaled, IsoVet®, Piramal Healthcare) and underwent surgery under sterile conditions as described previously [17]. Mice were euthanized at 12 h, 24 h, 2, 3, 15 and 28 days after femoral artery excision. Soleus and gastrocnemius (i.e., crural muscles) were dissected and processed for RNA, protein and histochemical analysis.

Experiments were performed following the European Communities Council Directives (2010/63/EU) guidelines for the care and use of laboratory animals and were approved by the Universidad de Navarra Animal Research Review Committee (Protocol numbers 093-09 and 036-19).

2.2. Histological analysis in mouse soleus

Soleus muscles were fixed for 24 h in 4% paraformaldehyde, dehydrated and embedded in paraffin, cut in 3 μm sections and immunostained with: rat anti-mouse F4/80 (Serotec), rat anti-mouse NIMP-R14 (Abcam), rat anti-mouse CD31 (Dianova), rabbit anti-human CXCR2 (Invitrogen), rabbit anti-mouse COL1A1 (LSBio), rabbit anti-mouse laminin (Sigma), rabbit anti-mouse NGAL (Invitrogen), and mouse anti-human αSMA (Dako) antibodies. Hematoxylin and eosin staining (H&E) was used to evaluate necrosis and the number of regenerating myofibers and Sirius red staining to analyze total collagen deposition.

Fluorescence *in situ* hybridization (FISH) [18] was used for miR-138-5p transcript assessment in WT soleus muscles at day 2 after ischemia using the anti-miR-138-5p (Qiagen, YD00612107-BCG) or scramble (Qiagen, YD00699004-BCG) locked nucleic acid (LNA) digoxigenin-conjugated probes.

2.3. Reverse target prediction (RTP) analysis for miRNA identification

To identify miRNAs involved in LCN2 regulation, an *in silico* reverse target prediction (RTP) analysis was performed using the www.targetscan.org web-based tool [19], yielding a list of miRNAs that potentially regulate human and murine *Lcn2* mRNAs. Subsequently, a subset of miRNAs was selected from this list of candidates; based on the differentially expressed genes identified from our previous RNA-Seq study in extracellular vesicles of PAD subjects (5). To ensure the biological relevance of the analysis, only those miRNAs predicted to interact with *Lcn2* mRNA and at least another gene from the RNA-Seq study were selected for further analysis.

2.4. Monocyte and macrophage stimulation

Human monocytes (THP-1) and murine macrophages (RAW 264.7), were cultured following ATCC protocols. THP-1 monocytes were stimulated with 500 ng/mL recombinant human LCN2 (Sigma) and harvested at baseline and 2- and 6-h after stimulation for RNA analysis.

RAW 264.7 cells were transfected with the miR-138-5p mimic (Qiagen) or the negative control miRNA mimic (Qiagen) using RNAiMAX lipofectamine (Thermo Fisher) and stimulated with 1 ng/mL lipopolysaccharide (LPS, Sigma) for 4 h and harvested for RNA analyses.

2.5. Isolation of mouse bone marrow derived macrophages

Mice were euthanized by CO_2 inhalation, femurs and tibias dissected, bone marrow cells flushed, and cultured for 7 days in differentiation medium to obtain bone marrow derived macrophages (BMDMs).

2.6. Flow cytometry

Blood samples were obtained by submandibular puncture at baseline, and at days 1 and 2 after HLI and immunostained with PE rat-anti mouse CD11b (BD Bioscience), APC rat anti-mouse Ly6G (BD Bioscience), FITC rat anti-mouse Ly6C (BD Bioscience), and PE-Vio770 rat anti-mouse CD115 (Miltenyi Biotec) antibodies. Flow cytometry was performed on a BD FACSCanto II flow cytometer (BD Biosciences) and results analyzed with FlowJo software (Tree Star Inc.).

2.7. Gene expression analyses in tissue, cells in culture and EVs

Total RNA from cell cultures was extracted using the semi-automated Maxwell RSC simplyRNA tissue kit (Promega) or from frozen mouse crural muscles (soleus and gastrocnemius) with TRIzol Reagent (Thermo Fisher). Prior to RNA isolation, EVs underwent pre-treatment with proteinase/RNase to eliminate co-precipitated free RNA. Then, total RNA was extracted using Direct-Zol RNA Miniprep kit (Zymo Research) following the manufacturer instructions. 1 μg of total RNA was reverse transcribed with random primers and Moloney murine leukemia virus reverse transcriptase (Thermo Fisher Scientific). For miRNAs, 5 ng of total RNA was retro-transcribed with stem-loop reverse transcription primers (Thermo Fisher Scientific) and MultiScribe reverse transcriptase enzyme (Thermo Fisher Scientific). qPCRs were performed on a ViiA 7 Real-Time PCR System (Thermo Fisher Scientific) using PrimeTime qPCR gene expression assays (IDT) for the protein-coding transcripts and TaqMan® MicroRNA Assays (Thermo Fisher Scientific) for the miRNAs (Supplemental Table 1). β-actin and GAPDH were used as housekeeping genes for mRNA analysis in mouse and human samples respectively. RNU6-1 (codifying for U6 snRNA) was used as reference gene to normalize miRNA readouts for mouse samples, and miR-103a for human

samples.

2.8. Preparation of LCN2 3′UTR constructs, molecular cloning, and luciferase assays

The online tool TargetScan was used to *in silico* predict the putative binding site of miR-138-5p (MIMAT0000430) within the *LCN2* 3′UTR. UCSC Genome Browser was consulted to obtain the 3′UTR oligonucleotide sequence of *LCN2* (NM_005564.5). Pme*I* (GTTT/AAAC) and Sal*I* (G/TCGAC) endonuclease restriction sites were inserted into the predicted sequences at 5′ and 3′ ends, respectively. In addition, Not*I* (GC/GGCCGC) site was inserted to further confirm oligonucleotide cloning into pmiRGLO Dual Luciferase miRNA Target Expression Vector (E1330, Promega, UK). Two LCN2 constructs were prepared including one containing either a wild-type or a mutant LCN2 3′UTR sequence (pLCN2 WT or pLCN2 MUT, respectively) downstream (3′) the firefly luciferase (FLuc). Customized *LCN2* WT or MUT sequences were purchased from Sigma-Aldrich. Heat shock transformation was used to amplify luciferase plasmid constructs in JM109 *E. coli*.

Endonuclease free luciferase plasmids were prepared (PLED35, GenElute™ Endotoxin-free Plasmid Midiprep Kit, Sigma-Merck). Lipofectamine LTX (15338030, Thermo Fisher, UK) was used to co-transfect pLCN2 constructs ± miR-138-5p mimic (YM00473517-ADA, Qiagen) and/or inhibitor (YI04102105-DDA, Qiagen) (both at 50 nM) into Raw264.7. Luciferase assays were performed after 24 h using a Dual-Glo® Luciferase Assay System (E2920, Promega, UK) following the manufacturer's instructions. All FLuc readouts were normalized to the internal control *Renilla* sp. luciferase (RLuc). An additional normalization to the control condition in each experiment was performed to avoid the data heterogeneity between experiments and reagents lot numbers. The data is shown as relative luminescence units (normalized to control).

2.9. Serum expression of miR-138-5p and LCN2 in patients with PAD and controls

PAD patients (n = 264) were enrolled at the outpatient service of the Department of Vascular Surgery, Hospital Universitario de Navarra (2010–2019). A thorough medical record was assembled for all patients. Controls (n = 54) were enrolled, and blood samples were collected at the time of clinical evaluation at the outpatient service of the Department of Internal Medicine, Clínica Universidad de Navarra (April 2016-December 2017).

The study was approved by the Institutional Review Boards of Hospital Universitario de Navarra (30/10) and Clínica Universidad de Navarra (2017/240), according to the standards of the Declaration of Helsinki on medical research. Written informed consent was obtained from all patients who were enrolled in this study (Supplemental materials and methods).

RNA isolation from serum was performed with the miRNeasy Serum/Plasma Advanced Kit (Qiagen, 217204). RNA was reverse transcribed, and amplified with the RT-PCR miRCURY LNA miRNA SYBR Green PCR kit using miRCURY LNA miRNA Custom PCR panels for miRNA-138-5p quantification. Panels included two house-keeping miRNAs: miR-191-5p and miR-103a-3p. miR-138-5p δCt was obtained as follows: miR-138-5p Ct - (the mean value of miR-191-5p and miR-103a-3p Cts). Serum miR-138-5p expression is presented as fold change relative to the miR-138-5p expression of control group.

LCN2 determination in serum was performed with the human Lipocalin-2/NGAL ELISA kit (Biovendor).

2.10. EVs separation from plasma and femoral artery plaque conditioned medium

EVs from plasma and femoral atherosclerotic plaques were separated as described previously [5]. Briefly, 800 μL of citrated platelet-free plasma were centrifuged twice at 20,000g for 70 min at 4 °C (Mikro 22R, Hettich Zentrifugen). Pelleted EVs were resuspended in 50 μL wash buffer (10 mM HEPES, 0.9% NaCl, pH = 7.4) and stored at −80 °C. Freshly collected femoral plaques were incubated for 24 h in culture medium [RPMI medium 1640 (Sigma), 2 mM L-Glutamine (Gibco, ThermoFisher), 1% penicillin/streptomycin (Sigma)]. Two mL of the resulting conditioned medium was centrifuged twice at 20,000g for 70 min at 4 °C to pellet EVs, that were resuspended in 100 μL wash buffer and stored at −80 °C.

2.11. Western blot analysis

Proteins from mouse tissues were extracted with RIPA buffer (Sigma) plus protease inhibitor cocktail (Roche), transferred onto nitrocellulose membranes (Bio-Rad) and incubated with: rabbit anti-CXCR2 (Invitrogen), rabbit anti-HIF-1α (Novus Biologicals), or rabbit anti-NGAL (Invitrogen, PA5-79590) antibodies.

2.12. Statistical analysis

Results are shown as median (IQR). Statistical significance was established as $p < 0.05$. The statistical analysis was performed in R environment (version 4.1.2) and with SPSS version 15.

3. Results

3.1. LCN2 expression is upregulated in the skeletal muscle early after hind limb ischemia

To assess the possible role of LCN2 in muscle recovery, its mRNA expression was measured in skeletal muscles (soleus and gastrocnemius) of WT mice at different time-points after femoral artery excision. As shown in Fig. 1A and B, and Supplemental Fig. 1, *Lcn2* mRNA and protein increased greatly, within the 48 h following ischemia, decreasing gradually as the muscle progresses in the reparative response. Moreover, morphological analysis showed the colocalization of Lcn2 with neutrophils, but not with macrophages, in soleus of WT mice 48 h post femoral ligation (Fig. 1C).

3.2. LCN2 deficiency modulates the early degenerative phase of skeletal muscle damage

Our results in WT mice suggested the possible participation of LCN2 in the processes triggered by tissue damage early after femoral artery ligation. Therefore, we performed hindlimb ischemia in WT and *Lcn2*$^{-/-}$ mice [16]. To test the hypoxia induction, we determined HIF-1α levels by western blot in crural muscles (soleus and gastrocnemius) before and after ischemia, observing an upregulation of HIF-1α 2- and 15-day post-surgery in both genotypes (Supplemental Fig. 2). Then, we studied the inflammatory response in blood and crural muscles (Fig. 2 and Supplemental Figs. 3 and 4).

In blood, leukocyte numbers (CD11b^{+}) rose similarly in WT and *Lcn2*$^{-/-}$ mice early after ischemia (Supplemental Fig. 4A). Likewise, granulocyte numbers (CD11b^{+}CD115^{-}Ly6G^{+}) rapidly increased following ischemia in both genotypes, but especially in the *Lcn2*$^{-/-}$ mice at days 1 and 2 (Fig. 2A, $p < 0.05$ *vs* WT in both time points). A significant interaction effect was found between genotype, sex, and time variables when analyzing circulating total (CD11b^{+}CD115^{+}), patrolling (CD11b^{+}CD115^{+}Ly6C^{low}) and proinflammatory monocyte subpopulations (CD11b^{+}CD115^{+}Ly6C^{high}), suggesting a sex-specific effect of Lcn2 in these cell types. As such, total circulating monocytes and patrolling cells were significantly reduced at day 2 post ischemia in *Lcn2*$^{-/-}$ males (Fig. 2B and C), whereas proinflammatory monocytes were higher (Fig. 2D). In females, no significant differences were found in total monocytes or their subpopulations between genotypes (Supplemental Figs. 4B–D).

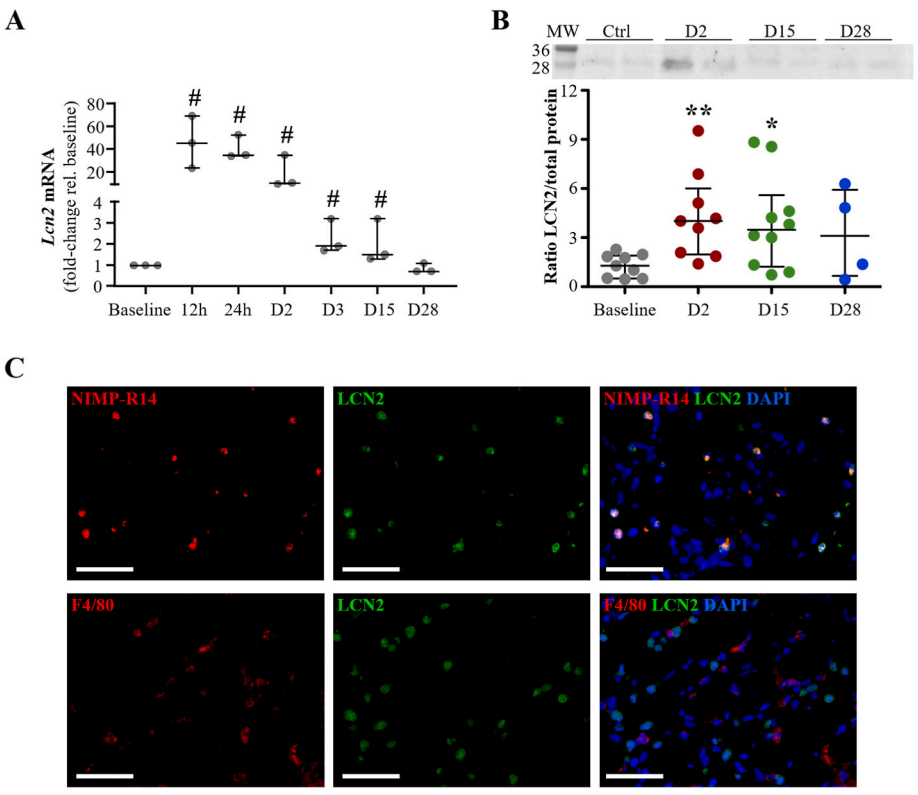

Fig. 1. LCN2 expression in wild-type (WT) skeletal muscle after hind limb ischemia.
(A) *Lcn2* mRNA was measured by RT-qPCR in the crural muscles (soleus and gastrocnemius) of WT mice before surgery (baseline) and at several time points after hind limb ischemia (12-, 24-, 48-h and 3-, 15-, 28-days). **β-actin** was used as housekeeping gene. Data are presented as fold change relative to baseline. n = 3 replicates/time point. #$p = 0.05$ *vs* baseline. (B) Representative Western blot and quantification for LCN2 in soleus and gastrocnemius muscles of WT mice before and after femoral artery ligation. Data are presented as ratio LCN2/total protein (n = 9–4). MW: Molecular weight marker (kDa). *$p < 0.05$ and **$p < 0.01$ *vs* baseline. (C) Double immunofluorescence for LCN2 and NIMP-R14 (neutrophils) or F4/80 (macrophages) was performed to determine the cellular origin of LCN2 in WT soleus muscles at day 2 post-ischemia. DAPI (in blue) was used as nuclear staining. Scale bar denotes 100 μm. (For interpretation of the references to colour in this figure legend, the reader is referred to the Web version of this article.)

The morphological analysis of the soleus muscles 2 days post-ischemia revealed a significant interaction between genotype and sex variables in the infiltrating neutrophils (NIMP-R14$^+$). *Lcn2*$^{-/-}$ males presented significantly higher neutrophil positive areas in the soleus (% neutrophil area/total area: 0.005 (0.005) WT *vs* 0.085 (0.072) *Lcn2*$^{-/-}$, $p = 0.006$, Fig. 2E), whereas no differences were found in females (Supplemental Fig. 4E). Conversely, macrophage (F4/80$^+$) content was reduced in the *Lcn2*$^{-/-}$ soleus compared to WT (Fig. 2F, $p = 0.049$), both in males and females.

3.3. *Inflammatory markers and chemokine expression in WT and Lcn2*$^{-/-}$ *crural muscles early after ischemia*

Our results suggest that LCN2 might modulate early systemic and local responses after ischemia. Therefore, several inflammatory markers were measured by qPCR in the crural muscles of both genotypes 48 h post-injury. A significant interaction between genotype and sex was found for TNFα, and two anti-inflammatory markers Arg1 and IL10, which were significantly elevated in the skeletal muscles of *Lcn2*$^{-/-}$ males (Fig. 3A), while no differences were found in females (Supplemental Table 2). To further investigate this phenotype, we isolated and differentiated BMDMs from WT and Lcn2−/− mice and determined the mRNA levels of different pro- and anti-inflammatory markers. *In vitro* and without further differentiation stimuli Lcn2 deficient BMDMs presented increased *Nos2* expression compared to WT ($p = 0.007$, Supplemental Table 3), while no differences in other pro- or anti-inflammatory markers were observed between the genotypes.

These data point towards a possible role of LCN2 in immune cell mobilization and recruitment into the injured skeletal muscle right after ischemia. Therefore, based on previous reports showing the effect of LCN2 on chemokine regulation [14,20,21], we determined the gene expression of several neutrophil and monocyte chemoattractants in skeletal muscles of both genotypes. The mRNA expression of the neutrophil chemokine *Cxcl1* was significantly increased ($p < 0.001$) in *Lcn2*$^{-/-}$ mice muscles compared to WT at day 2, while a similar trend, but no significant, was observed for *Cxcl2* ($p = 0.083$, Fig. 3B). As for their receptor, an interaction between genotype and sex was detected, resulting in a significant upregulation of *Cxcr2* mRNA in *Lcn2*$^{-/-}$ males, but not in females (Fig. 3C), with a similar trend at protein level (Fig. 3D and Supplemental Figs. 5A and B). Of note, immune staining of the ischemic muscles revealed that Cxcr2 was mainly expressed by neutrophils (NIMP-R14) and macrophages (F4/80) (Fig. 3E). In contrast, the monocyte chemokine *Ccl5* was significantly decreased in *Lcn2*$^{-/-}$ muscle compared to WT at day 2 (Fig. 3F), whereas no differences were observed in *Ccl2* and *Ccr2*. These data suggest that LCN2 might modulate neutrophil and monocyte chemotaxis through *Cxcr2* and *Ccl5* pathways.

To assess whether Lcn2 deficiency constitutively regulated Cxcr2 in immune cells, its levels were measured by flow cytometry in bone marrow derived granulocytes (CD45$^+$Ly6G$^+$) and monocytes (CD45$^+$Ly6C$^+$) of non-operated WT and *Lcn2*$^{-/-}$ mice. In these conditions, no differences in Cxcr2 levels were observed between the genotypes either in granulocytes or monocytes (Supplemental Fig. 5C), suggesting that the regulation of Cxcr2 by Lcn2 in immune cells might be primarily exerted upon muscle damage.

To test our hypothesis that LCN2 could modulate the expression of

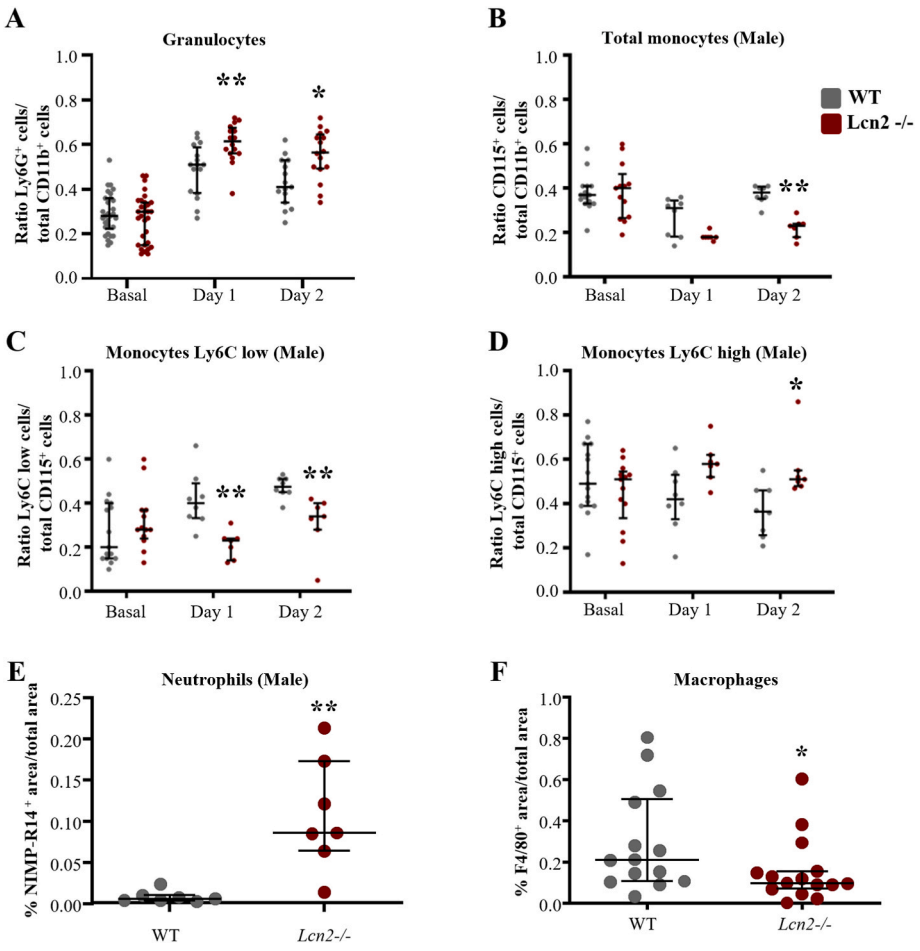

Fig. 2. Systemic and local inflammatory response to hypoxia in WT and LCN2 deficient mice.
(A) Circulating granulocytes (CD11b + CD115- Ly6G+) were increased in *Lcn2*$^{-/-}$ mice 24, and 48 h post-ischemia. (B-D) Total monocytes (CD11b + CD115+), Ly6C low (C) and Ly6C high monocytes (D) of male mice. Blood samples were drawn from all mice at baseline (n = 31) and the number decreases as mice are euthanized at days 1 and 2. n = 8–6 mice/genotype/time point, two independent experiments. *$p < 0.05$ **$p < 0.01$ *vs* WT at the same time point. Data were $\log_{10}$-transformed for the statistical analysis and are presented as median (IQR). (E) Soleus muscle infiltrating neutrophils (NIMP-R14) are increased in *Lcn2*$^{-/-}$ male mice 2 days post-injury. (F) Macrophage (F4/80) content was reduced upon LCN2 deficiency at day-2 after surgery, regardless mice sex. n = 16–14 mice/genotype, two independent experiments. *$p < 0.05$ **$p < 0.01$ *vs* WT.

chemoattractants and their receptors, a human monocytic (THP-1) cell line was stimulated with recombinant human (rh)LCN2. Two hours after treatment *Cxcr2* expression was reduced by 28% (Fig. 3G, $p < 0.01$), while no differences in *Cxcl1*, *Cxcl2*, *Ccl2*, *Ccl5* or *Ccr2* were observed (Supplemental Fig. 6).

3.4. LCN2 deficiency delays skeletal muscle regeneration

The reparative phase of muscle regeneration greatly depends on the mechanisms activated by ischemia during the degenerative phase, and deficiencies at the beginning of this process can hamper tissue regeneration at later stages. Based on the observed differences in the inflammatory response upon Lcn2 deficiency, we performed morphological studies 15 days post-injury to address changes in myocyte regeneration, angio- and arterio-genesis, and collagen deposition (Supplemental Fig. 7). As shown in Table 1, 15 days post-ischemia *Lcn2*$^{-/-}$ mice presented increased numbers of smaller and central nucleated myocytes in soleus compared to WT mice ($p = 0.040$), that was accompanied by a non-significant elevation in myocyte density ($p = 0.066$) and a moderated decrease in their size ($p = 0.081$). In addition, knockout muscles showed a significant enhancement in α-SMA positive arterioles ($p = 0.025$), a trend for elevated vessel density ($p = 0.130$), and a non-significant accumulation of total collagen and type I collagen deposits, suggesting that in the absence of Lcn2 there is a delay in muscle regeneration and arteriogenesis. No sex-specific responses were detected in these analyses.

3.5. Regulation of Lcn2 mRNA by microRNAs in skeletal muscle after ischemia

To identify the miRNAs involved in LCN2 regulation, an *in silico* reverse target prediction analysis was performed using the web-based tool www.targetscan.org. To ensure the biological relevance of the predicted miRNAs, we selected a subset of miRNAs that could target *Lcn2* and at least one other mRNA potentially involved in PAD pathophysiology. To this end, the analysis was based on a list of 15 transcripts previously identified by our group as differentially expressed in EVs of PAD patients compared with control subjects (Supplemental Table 4) [5]. The reverse target prediction analysis performed for human and murine LCN2, rendered several miRNA candidates for the human and/or murine transcripts (Supplemental Table 5). Among them, miR-138-5p was the only predicted candidate with a conserved target site in human and murine *Lcn2*, and thus, it was the one selected for further analysis.

To determine whether miR-138-5p was altered upon skeletal muscle ischemia, its expression was measured by RT-qPCR in crural muscles of

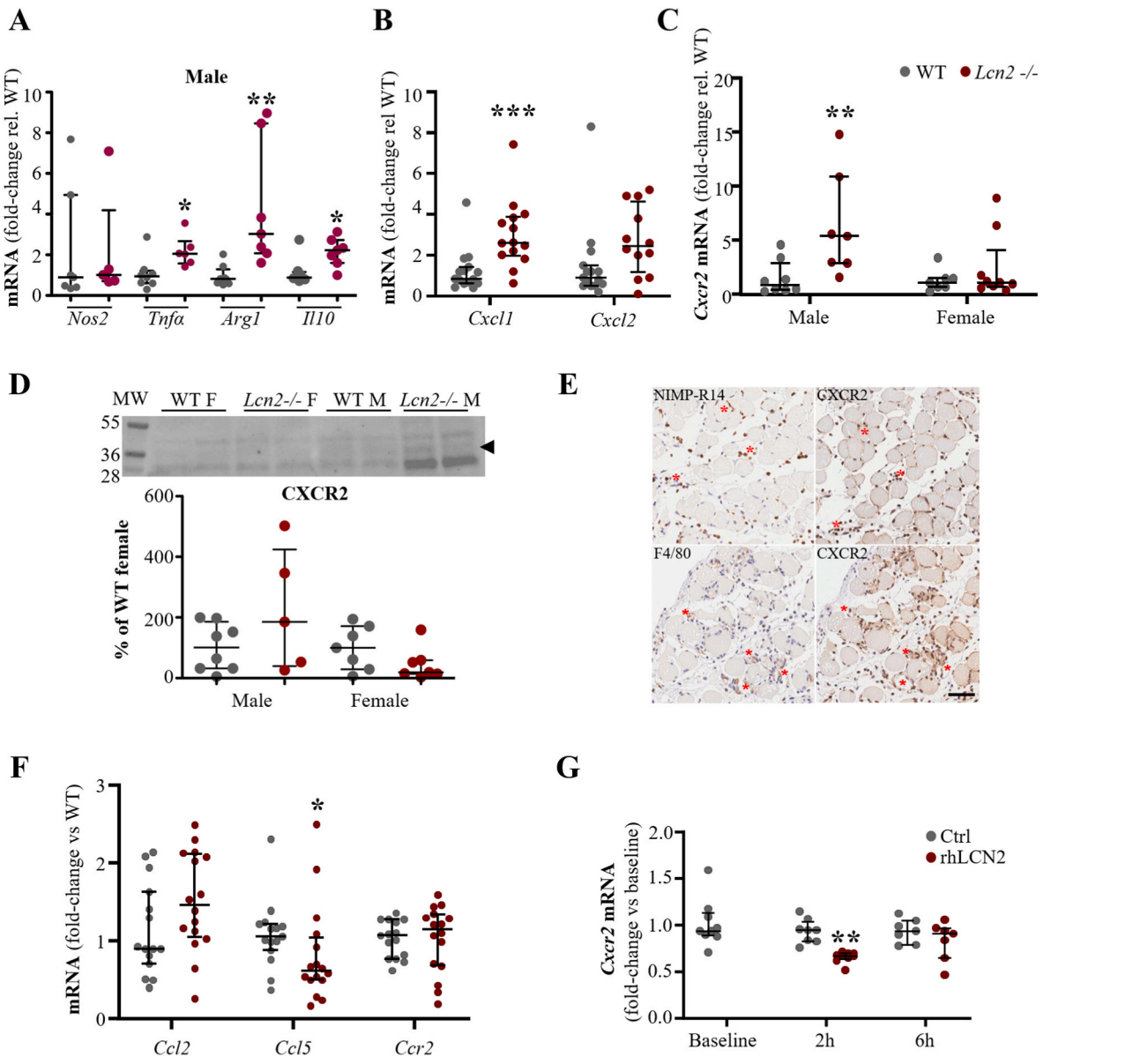

Fig. 3. Expression of neutrophil and monocyte chemoattractants in skeletal muscle of WT and LCN2 deficient mice, and *in vitro* modulation by LCN2.
(A, B and C) Pro- and anti-inflammatory markers (A), neutrophil chemokines *Cxcl1*, *Cxcl2* (B) and *Cxcr2* (C) mRNA levels measured by RT-qPCR in soleus and gastrocnemius muscles of WT and *Lcn2*$^{-/-}$ mice at day-2 after ischemia. *β-actin* was used as housekeeping gene. Data are presented as fold change relative to WT. n = 15–16 mice/genotype. (D) Western blot for CXCR2 in crural muscles at day 2. The arrow points to the monomeric form of CXCR2 (≈40 kDa). CXCR2 expression was corrected by total protein. Data are presented as percentage of WT female. n = 5–8 mice/genotype/sex. F; female, M; Male, MW; Molecular weight (kDa). (E) Immunohistochemistry for neutrophils (NIMP-R14), macrophages (F4/80), and CXCR2 in consecutive soleus tissue slides of WT mice at day 2 post-ischemia. Red asterisks indicate similar tissue regions. Scale bar denotes 50 μm. (F) mRNA expression of *Ccl2*, *Ccl5* and *Ccr2* 2 days after ischemia in crural muscle. β-actin was used as housekeeping gene. Data are presented as fold change relative to WT. n = 15–16, two independent experiments. *$p < 0.05$ **$p < 0.01$ ***$p < 0.001$ vs WT. Data were log10-transformed for the statistical analysis and are shown as median (IQR). (G) mRNA expression of *Cxcr2* in THP-1 monocytes at baseline and 2- and 6-h after rhLCN2 (500 ng/mL) stimulation. GAPDH was used as housekeeping gene. Data are presented as fold change relative to baseline. n = 7–9 replicates/treatment/time point, three independent experiments. **$p < 0.01$ *vs* control (vehicle) at the same time point. Data are shown as median (IQR). (For interpretation of the references to colour in this figure legend, the reader is referred to the Web version of this article.)

WT mice at different time-points after femoral artery excision, showing a progressive reduction from 12 to 48 h post-surgery (Fig. 4A). Conversely, its levels increased at day-3 (40-fold) and remained upregulated at days 15 and 28 (70-fold) compared to baseline. Notably, miR-138-5p and *Lcn2* mRNA displayed opposite expression pattern, showing a significant inverse correlation (rho = -0.58, $p = 0.005$), which suggests that *Lcn2* may be post-transcriptionally regulated by miR-138-5p *in vivo*. The expression of miR-138-5p was also verified by *in situ* hybridization in WT soleus at day-2 post-ischemia. As shown in Fig. 4B, early after ischemia, miR-138-5p could be still detected in the infiltrating cells surrounding damaged myofibers.

In vitro experiments were performed in a murine macrophage cell line to determine the possible regulation of *Lcn2* by miR-138-5p. RAW 264.7 cells were transfected with a miR-138-5p mimic or a negative control miRNA mimic, after which, the expression of *Lcn2* mRNA was induced by incubation with LPS. As shown in Fig. 4C, miR-138-5p mimic decreased the expression of *Lcn2* transcript by 50% compared to untreated cells, and by 30% compared to cells transfected with the negative control miRNA mimic ($p = 0.009$ for both).

In silico predictions revealed a putative binding site of miR-138-5p

Table 1
Muscle regeneration, neovascularization and fibrosis in wild-type (WT) and *Lcn2*$^{-/-}$ mice at day 15 post-ischemia.

	WT (n = 12–15)	*Lcn2*$^{-/-}$ (n = 11–14)	*p*
Regenerating myocytes (%)	13(43)	72(69)	**0.040**
Myocyte size (μm^2)	784(387)	606(322)	0.081
Myocyte/mm^2	629(333)	963(499)	0.066
CD31$^+$ vessels/mm^2	1015(411)	1270(534)	0.130
αSMA + arterioles/mm^2	17(11)	28(13)	**0.025**
Collagen/total area (%)	4(3)	6(3)	0.499
Collagen type I/total area (%)	6.5(9)	9.4(17)	0.124

Data are shown as median (IQR).

on Lcn2 3′UTR (position 25-31). Previous publications have confirmed such binding in HEK293 cells [22]. To further explore whether miR-138-5p regulates Lcn2 by complementary hybridization of the predicted site in a relevant cell model, luciferase assays were additionally performed. RAW 264.7 macrophages were co-transfected with dual luciferase reporter gene vector for the WT LCN2 (pLCN2 WT) or a mutant (pLCN2 MUT) at the binding site with miR-138-5p, together with the miR-138-5p mimic and/or the inhibitor. As shown in Fig. 4D (left panel), the miR-138-5p mimic reduced by 25% the firefly luciferase activity of the pLCN2 WT ($p = 0.037$). No effect was seen for the miR-138-5p inhibitor or its combination with miR-138-5p mimic. We also reported that miR-138-5p reduces the expression of mutant Lcn2 sequence by 5% (Fig. 4D right panel, $p = 0.014$), which may suggest some unspecific binding to the Lcn2 constructs. We cannot rule out whether miR-138-5p may bind to additional sites within *Lcn2*. Indeed, miRWalk *in silico* tool predicts a binding site within the Lcn2 5′UTR that could also contribute to the significant down-regulation elicited by miR-138-5p mimic experiments above.

3.6. Serum expression of miR-138-5p and LCN2 levels in PAD are inversely associated

Finally, to determine a possible relationship between the expression of miR-138-5p and LCN2 in a clinical context, we determined serum levels of both molecules in patients with PAD and healthy controls (n = 264, 88% male, mean age 71 years, and n = 54, 76% male, mean age 69, respectively, Supplemental Table 6 and Supplemental Fig. 8).

Pearson correlation analysis of the complete population revealed a negative inverse association between miR-138-5p expression (presented as fold change relative to control) and LCN2 concentration (n = 318, r = -0.186, $p = 0.001$). This was further confirmed by linear regression analysis showing a significant inverse association between circulating LCN2 levels and miR-138-5p expression before and after adjusting by other cardiovascular risk factors including eGFR (Table 2, $p \leq 0.001$).

When dividing the population according to vascular pathology, PAD patients presented a reduction in serum miR-138-5p expression compared with controls (median (IQR) fold change: 1.00 ± 0.97 controls *vs* 0.78 ± 1.40 PAD, $p = 0.008$, Fig. 4E), together with an increase in LCN2 levels (median (IQR) ng/mL: 54(19) controls *vs* 90(60) PAD, $p < 0.001$). Binary logistic regression analysis confirmed the association between low levels of miR-138-5p and PAD before and after correcting by other confounding factors (OR: 0.63, (95% IC, 0.43–0.93), $p = 0.02$, model 2, Supplemental Table 7), and between high levels of LCN2 and PAD (OR: 1.04, (95% IC, 1.03–1.07), $p \leq 0.001$, model 2, Supplemental Table 8).

To further investigate the circulating sources of miR-138-5p in PAD, we determined its expression in plasma EVs, and locally, in femoral plaques, as well as in femoral plaques-derived EVs. As shown in Fig. 4F, miR-138-5p was detected in plasma EVs, although not in all tested samples, and in femoral plaques and in their derived EVs (Fig. 4G), suggesting the potential contribution of atherosclerotic lesions to the systemic expression of miR-138-5p. *LCN2* mRNA and protein were also harbored by circulating EVs, and by EVs from femoral plaque-conditioned medium (Supplemental Fig. 9).

4. Discussion

In this study we found that LCN2 deficiency resulted in an enhanced systemic and local inflammatory response at the degenerative phase of skeletal muscle repair, and in a delayed muscle regeneration at the reparative phase. Early after ischemia the morphological changes induced by Lcn2 deficiency were accompanied by increased expression of proinflammatory markers and neutrophilic chemokines in crural muscles, and appeared to be sex-specific, predominantly affecting male mice. Finally, we identified miR-138-5p as a potential regulator of Lcn2 in a murine model of hindlimb ischemia, and found an inverse association between serum levels of miR-138-5p and LCN2 in patients with PAD.

We found that early after femoral artery ligation, *Lcn2*$^{-/-}$ mice presented increased blood and tissue neutrophils, while total monocytes and macrophages remained similar or reduced compared to WT. Interestingly, this was accompanied by a local deregulation in proinflammatory markers and chemokines. As such, *Lcn2*$^{-/-}$ crural muscle presented increased levels of the neutrophilic chemokines *Cxcl1*, *Cxcl2* and their receptor Cxcr2, which may favor the accumulation of neutrophils. Moreover, Cxcr2 expression was not altered in bone marrow immune cells at baseline, probably because Lcn2 is only functional when released from intracellular granules upon cell activation, for example, by ischemia [23]. In addition, *Ccl5* expression was lower in *Lcn2*$^{-/-}$ muscles, which might account for the reduced infiltrating macrophages observed in the soleus, despite the increased levels of proinflammatory monocytes (Ly6C^{high}) in blood. Regardless of current efforts, the role of LCN2 in inflammation remains controversial. For instance, 2 research groups reported dissimilar results in murine atherosclerosis models; Amersfoort J et al., reported larger plaques in *Ldlr*$^{-/-}$*Lcn2*$^{-/-}$ mice compared to *Ldlr*$^{-/-}$ at early stages of atherogenesis, observing no differences in advanced lesions [9], while, Fernandez-Garcia C.E. et al. described smaller plaques in *ApoE*$^{-/-}$*Lcn2*$^{-/-}$ arteries compared to *ApoE*$^{-/-}$, and the beneficial effect of an anti-LCN2 antibody decreasing lesion areas [8]. Several evidences argue towards a role of LCN2 to restrain inflammation. As such, in a model of pneumonia, *Lcn2*$^{-/-}$ lungs presented exacerbated neutrophil infiltration [24], and *in vitro*, LPS treatment increased the expression of proinflammatory markers in *Lcn2*$^{-/-}$ BMDMs [25]. Concomitantly, the administration of LCN2 upon bacterial infection induced a M2 phenotype in WT BMDMs [24]. In contrast to these data, a proinflammatory role for LCN2 has also been reported in other experimental models, [26–28]. For instance, in a model of abdominal aortic aneurysm, genetic or pharmacological neutralization of LCN2 reduced aortic expansion and neutrophil infiltration, and preserved smooth muscle cell integrity [29]. Other authors found similar phenotypes in livers of non-alcoholic steatohepatitis mice, and in hearts after myocardial infarction, where Lcn2 deficiency resulted in a reduction of neutrophil and macrophage infiltration, and decreased expression of proinflammatory genes, including Cxcr2 and Cxcl2 [14,30]. Furthermore, the short-term stimulation of BMDMs with recombinant LCN2 induced M1 phenotype *in vitro* [27]. Based on these results, it seems that the biological effects of LCN2 may depend on the stimulus triggering inflammation, and/or on the type of damage, either chronic or acute.

In our study, many of the observed differences between genotypes were only present in male but not female mice. These sex-specific effects occurred early after ischemia but were not detected during the muscle regeneration stage, indicating a probable involvement of sex-specific factors that modulate LCN2 response shortly after damage. In this regard, LCN2 expression can be regulated by the estrogen receptors (ER)α and ERβ, which inhibit or induce its expression, respectively [31]. In turn, LCN2 is reported to repress ERα expression [32]. This reciprocal interaction between LCN2 and ER signaling could possibly explain its sex-specific phenotype. For example, Lcn2 overexpression promoted the

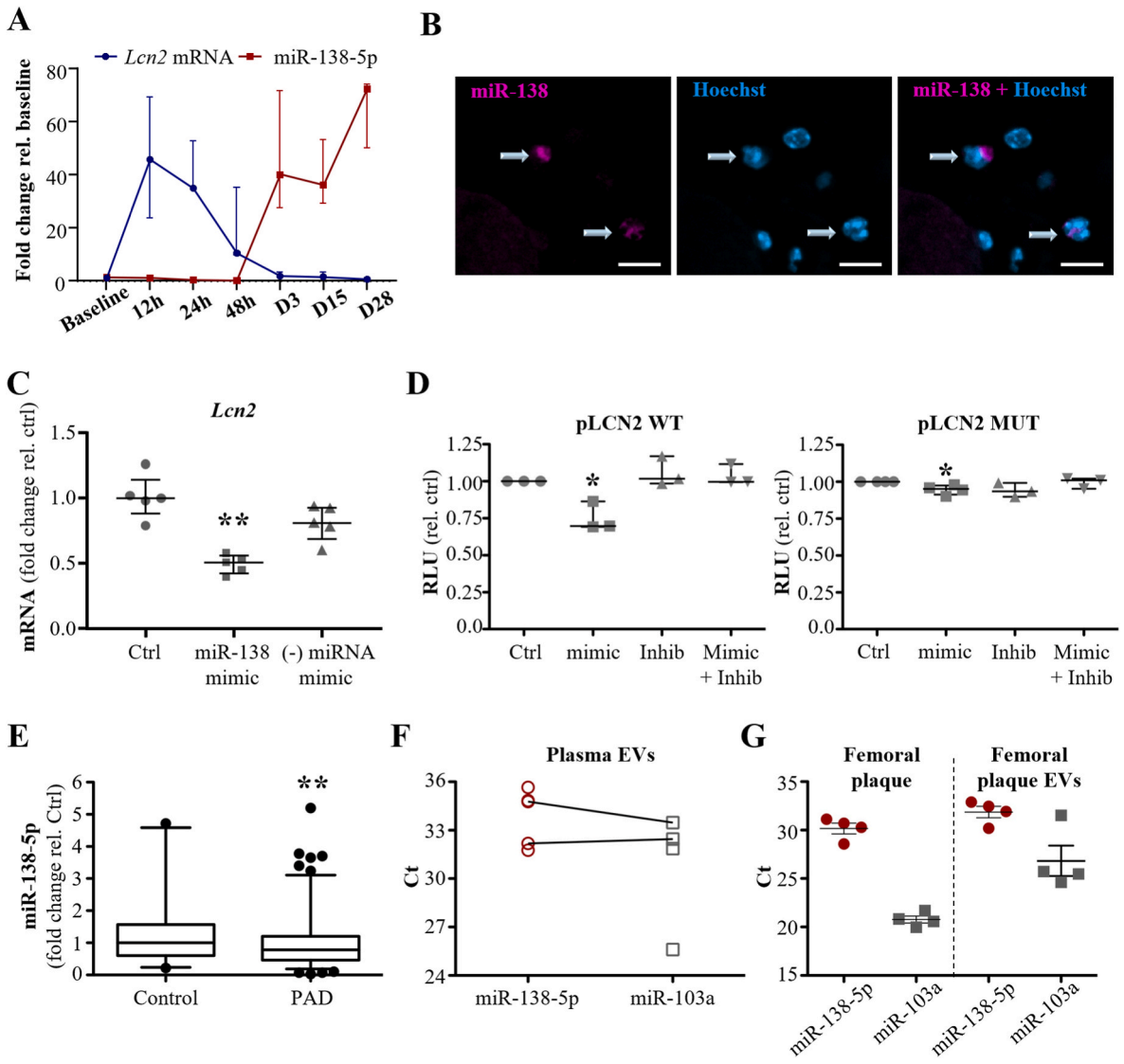

Fig. 4. Lcn2 and miR-138-5p expression *in vivo* and *in vitro*.
(A) miR-138-5p and *Lcn2* mRNA expression was measured in the ischemic muscles of WT mice at baseline and several time points after HLI (12-, 24-, 48-h and 3-, 15-, 28-days). *β-actin* was used as housekeeping gene for *LCN2* and *snU6* for miR-138-5p. Data are presented as fold change relative to baseline. n = 3 mice/time point, one experiment. (B) *In situ* hybridization of miR-138-5p (pink) in soleus muscle of WT mice at day-2 after surgery. Nuclei are shown in blue. Scale bar denotes 10 μm. (C) Macrophage cell line (RAW 264.7) was transfected with or without miR-138-5p mimic or negative control miRNA mimic (5 nM), and stimulated with LPS (1 ng/mL) to induce Lcn2 expression. *Lcn2* mRNA levels were measured by RT-qPCR. *β-actin* was used as housekeeping gene. Data are presented as fold change relative to control. n = 5 replicates/condition, performed in triplicate. $^{**}p < 0.01$ *vs* negative control and non-stimulated control. (D) RAW 264.7 cells were co-transfected with either pLCN2 WT (left panel) or pLCN2 MUT (right panel) and miR-138-5p mimic (mimic) and/or the inhibitor (inhib). Luciferase activity in cell lysates was measured 24 h later. Data are presented as relative luminescence units (RLU) normalized to control condition. n = 3–4 independent experiments/5 replicates/condition. $^{*}p < 0.05$ *vs* control (Ctrl). (E) miR-138-5p expression in serum of control subjects (n = 54) and PAD patients (n = 264). miR-191-5p and miR-103a-3p were used as housekeeping miRNAs. The expression of miR-138-5p is presented as fold change relative to control. Data are shown as median (IQR) and outliers. $^{**}p < 0.01$ *vs* control. (F) miR-138-5p expression in plasma EVs from PAD patients determined by RT-qPCR. miR-103a was included as housekeeping gene (n = 7). (G) miR-138-5p expression in human femoral plaques and in EVs isolated from femoral plaques conditioned medium. miR-103a was included as housekeeping gene (n = 4). (For interpretation of the references to colour in this figure legend, the reader is referred to the Web version of this article.)

upregulation of inflammatory and fibrotic genes in the adipose tissue of *Lcn2*$^{-/-}$ female mice, but not in males [32]. Unfortunately, from our study we are not able to elucidate the exact molecular mechanisms behind the observed sex-specific phenotype.

At the regenerative phase of muscle repair, day 15 in our model, *Lcn2*$^{-/-}$ deficient mice displayed a delayed phenotype as compared to WT soleus muscles, with increased regenerating myofibers, incomplete angio- and arteriogenic responses, and a non-significant accumulation of collagen in soleus. These results agree with previous data describing an impaired skeletal muscle repair in response to toxin injury in Lcn2−/− mice which was accompanied by a reduced satellite cell activation [13]. Moreover, Lcn2−/− mice also presented increased muscle fibrosis likely through a reduction in MMP-9 activity [13]. These results however, are in apparent contradiction with those obtained in murine models of hypertension and myocardial infarction where the inhibition of LCN2 reduced vascular and cardiac fibrosis [33,34], suggesting a tissue and/or injury specific activity of LCN2. The role of LCN2 in angiogenesis also shows diverging effects that depend on the applied cell type and stimuli [29,35–37]. For instance, LCN2 presented a pro-angiogenic role in mice via upregulation of the vascular endothelial growth factor [35], whereas LCN2 overexpression led to a reduced microvessel density in a mice model of pancreatic cancer [37].

Table 2
Linear regression analysis to explore the association between serum miR-138-5p and LCN2 levels before and after correcting by other CV risk factors (n = 318). Dependent variable LCN2.

	B(95% CI)	*p*
Univariable		
miR-138-5p (fold-change)[a]	−0.131(-0.207 to −0.054)	0.001
Multivariable		
Age (years)	−0.005(-0.008 to −0.003)	<0.001
Gender (male)	0.088(0.025–0.150)	0.006
Smoker (yes/no/ex)	−0.026(-0.052 to 0.001)	0.058
Diabetes mellitus (yes)	0.005(-0.037 to 0.047)	0.812
Dyslipidemia (yes)	−0.069(-0.114 to −0.024)	0.003
eGFR (mL/min/1.73m^2)	−0.005(-0.006 to −0.003)	<0.001
hs-CRP (mg/L)[a]	0.138(0.103–0.172)	<0.001
miR-138-5p (fold-change)[a]	−0.130(-0.193 to −0.067)	<0.001

[a] Logarithmically transformed variables. eGFR: estimated-glomerular filtration rate.

miRNAs, a class of small noncoding RNAs, are essential post-transcriptional regulators of gene expression, and emerge as novel biomarkers and therapeutic targets in the cardiovascular field [38]. To identify the miRNAs potentially targeting LCN2 we performed an *in silico* reverse target prediction analysis for human and murine *Lcn2* 3′UTR and found several miRNA candidates for human and mouse, being miR-138-5p the only conserved regulator in both species. Based on the coincident prediction for mouse and human, on previous studies describing a possible role of miR-138-5p in promoting endothelial dysfunction [39,40] and cardiomyocyte apoptosis *in vitro* [41], and on the observed downregulation of miR-138-5p in peripheral blood mononuclear cells of PAD patients *vs.* healthy controls [42,43], we decided to narrow our study to miR-138-5p. By doing so, we found an inverse correlation between the levels of miR-138-5p and *Lcn2* mRNA in ischemic WT skeletal muscles over time, suggesting a possible relationship between the miRNA and its potential target. *In vitro*, we observed a partial reduction of *Lcn2* mRNA and a decrease in luciferase activity by the miR-138-5p mimic in murine macrophages, indicating the interaction between the regulator and its target, as already described by others [22,44]. In a clinical situation, we were able to confirm a downregulation of miR-138-5p in serum of PAD patients compared with controls [42,43]. More interesting, this was accompanied by an increase in blood LCN2 levels, further reinforcing its possible role as one of the post-transcriptional regulators of this specific target. Our *in vivo* and human results point towards a contribution of the skeletal muscles, and the vasculature to the systemic expression of miR-138-5p and LCN2, being in part encapsulated/carried in EVs. Overall, these findings suggest that miR-138-5p may be likely involved in the regulation of LCN2 after skeletal muscle ischemia in mice, and in PAD patients. As such, this miRNA could represent a promising target for future therapies aiming to modulate LCN2, although as suggested by the reverse target prediction analysis, its regulation might not be exclusive to miR-138-5p.

Study limitations: The role of LCN2 in PAD pathophysiology was evaluated using a murine HLI model which, although commonly used, does not precisely mimic PAD progression in humans. The acute ischemic damage induced in this model greatly differs from the chronic nature of PAD. The gradual occlusion of the arteries in PAD patients allows the distal skeletal muscles to slowly adapt to the reduced oxygen and nutrient conditions [45]. Likewise, the gradually increasing shear stress allows longer period of collateral vessel formation compared to the rapid blood flow changes induced in the HLI model [46]. In addition, the presence of cardiovascular risk factors and atherosclerosis in PAD subjects but not in the current HLI model, should also be considered as a limitation of this study. In the clinical study 88% of PAD patients and 76% of control subjects were male, therefore, no reliable sub-analysis to check differences in miR-138-5p or circulating LCN2 levels between male and female patients could be performed. The high Ct readouts of miR-138-5p reported in blood and EVs from patients (Supplemental Figure 8 and Fig. 4F) could limit the clinical impact of our findings. Nevertheless, the multiple quality control tests, intra-sample reproducibility and the number of clinical samples successfully assayed confer robustness to our findings. Previous publications have shown that most abundant EV-derived miRNAs may peak at Ct 31-35, still with relevant biological impact [47]. Future research on the role of miR-138-5p on atherosclerosis manifestations and vascular beds would be required to reveal its impact in such a complex and multifactorial disease.

4.1. Conclusions

This study reports a possible dual role for LCN2 in acute and chronic pathophysiological conditions (Fig. 5). Likewise, a sex-specific function of LCN2 in the regulation of the early systemic and local inflammatory response can be inferred. Our data reinforce a possible activity of LCN2 as a repressor in acute inflammatory conditions, while promoting vascular disfunction in chronic systemic low-grade inflammatory contexts. Moreover, we present miR-138-5p as one potential post-transcriptional regulator of LCN2 *in vivo*, in skeletal muscle of mice, and in atherosclerotic plaques and serum of PAD patients, emerging as a new target for future studies aiming to modulate LCN2 in PAD pathophysiology.

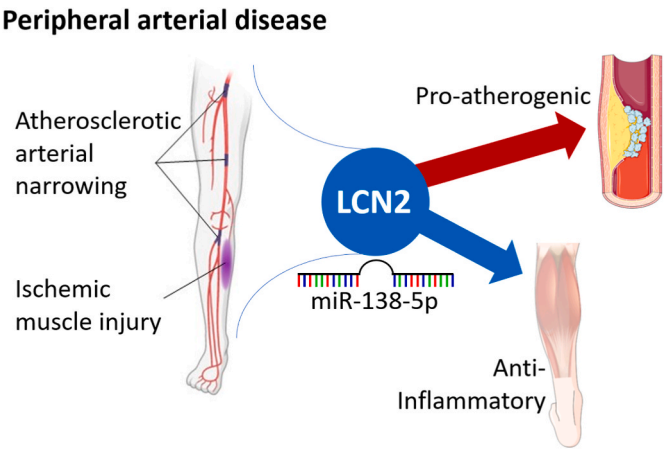

Fig. 5. Possible dual role of LCN2 in lower limb PAD.
Our results reinforce a probable role of LCN2 in restraining inflammation early after skeletal muscle ischemia, while being associated with vascular damage in PAD, and identifies miR-138-5p as one potential post-transcriptional regulator of LCN2.

Financial support

The Foundation for Applied Medical Research, Universidad de Navarra (Spain); the Ministry of Science and Innovation, Institute of Health Carlos III, co-funded by the European Fund for Economic and Regional Development (FEDER) [PI18/01195], This research was supported by CIBER -Consorcio Centro de Investigación Biomédica en Red-Cardiovascular (CB16/11/00483 and CB16/11/00333), Instituto de Salud Carlos III, Ministerio de Ciencia e Innovación. Virto Group (Spain). This work was supported by a Short-Term Scientific Mission from COST Action CA17129 funded by COST (European Cooperation in Science and Technology).

CRediT authorship contribution statement

Goren Saenz-Pipaon: Conceptualization, Data curation, Formal analysis, Investigation, Methodology, Writing – original draft, Writing – review & editing. **Eva Jover:** Formal analysis, Methodology, Writing – review & editing. **M. Leontien van der Bent:** Methodology, Writing – review & editing. **Jose A. Rodriguez:** Writing – review & editing. **Amaya Fernández-Celis:** Formal analysis, Methodology. **Paul H.A. Quax:** Writing – review & editing. **Jose A. Paramo:** Writing – review & editing. **Natalia López-Andrés:** Writing – review & editing. **Jose Luis Martín-Ventura:** Writing – review & editing. **Anne Yaël Nossent:** Data curation, Formal analysis, Methodology, Writing – review & editing. **Carmen Roncal:** Conceptualization, Data curation, Formal analysis, Investigation, Methodology, Supervision, Writing – original draft, Writing – review & editing.

Declaration of competing interest

The authors declare that they have no known competing financial interests or personal relationships that could have appeared to influence the work reported in this paper.

Acknowledgments

We particularly acknowledge the patients for their participation and the Biobank of the University of Navarra for its collaboration. We want to thank Lara Montori and Miriam Belzunce for their technical assistance (Laboratory of Atherothrombosis, Cima Universidad de Navarra).

Appendix A. Supplementary data

Supplementary data to this article can be found online at https://doi.org/10.1016/j.atherosclerosis.2023.117343.

References

[1] U. Frank, S. Nikol, J. Belch, V. Boc, M. Brodmann, P.H. Carpentier, A. Chraim, C. Canning, E. Dimakakos, A. Gottsäter, C. Heiss, L. Mazzolai, J. Madaric, D. M. Olinic, Z. Pécsvárady, P. Poredoš, I. Quéré, K. Roztocil, A. Stanek, D. Vasic, A. Visonà, J.-C. Wautrecht, M. Bulvas, M.-P. Colgan, W. Dorigo, G. Houston, T. Kahan, H. Lawall, I. Lindstedt, G. Mahe, R. Martini, G. Pernod, S. Przywara, M. Righini, O. Schlager, P. Terlecki, ESVM Guideline on peripheral arterial disease, Vasa 48 (2019) 1–79, https://doi.org/10.1024/0301-1526/a000834.

[2] V. Aboyans, J.B. Ricco, M.L.E.L. Bartelink, M. Björck, M. Brodmann, T. Cohnert, J. P. Collet, M. Czerny, M. De Carlo, S. Debus, C. Espinola-Klein, T. Kahan, S. Kownator, L. Mazzolai, A.R. Naylor, M. Roffi, J. Röther, M. Sprynger, M. Tendera, G. Tepe, M. Venermo, C. Vlachopoulos, I. Desormais, P. Widimsky, P. Kolh, S. Agewall, H. Bueno, A. Coca, G.J. De Borst, V. Delgado, F. Dick, C. Erol, M. Ferrini, S. Kakkos, H.A. Katus, J. Knuuti, J. Lindholt, H. Mattle, P. Pieniazek, M. F. Piepoli, D. Scheinert, H. Sievert, I. Simpson, J. Sulzenko, J. Tamargo, L. Tokgozoglu, A. Torbicki, N. Tsakountakis, J. Tuñón, M.V. De Ceniga, S. Windecker, J.L. Zamorano, E. Barbato, I.M. Coman, V. Dean, D. Fitzsimons, O. Gaemperli, G. Hindricks, B. Iung, P. Juni, P. Lancellotti, C. Leclercq, T. McDonagh, P. Ponikowski, D.J. Richter, E. Shlyakhto, I.A. Simpson, P. H. Zelveian, M. Haumer, D. Isachkin, T. De Backer, M. Dilic, I. Petrov, M. V. Kirhmajer, D. Karetova, E. Prescott, H. Soliman, A. Paapstel, K. Makinen, S. Tosev, E. Messas, Z. Pagava, O.J. Müller, K.K. Naka, Z. Járai, T. Gudjonsson, M. Jonas, S. Novo, P. Ibrahimi, O. Lunegova, V. Dzerve, N. Misonis, J. Beissel, E. Pllaha, M. Taberkant, T. Bakken, R. Teles, D. Lighezan, A. Konradi, M. Zavatta, J. Madaric, Z. Fras, L.S. Melchor, U. Näslund, B. Amann-Vesti, A. Obiekezie, ESC guidelines on the diagnosis and treatment of peripheral arterial diseases, in collaboration with the European society for vascular surgery (ESVS), 2018, Eur. Heart J. 39 (2017) 763–816, https://doi.org/10.1093/eurheartj/ehx095.

[3] B. Rantner, B. Kollerits, J. Pohlhammer, M. Stadler, C. Lamina, S. Peric, P. Klein-Weigel, H. Mühlthaler, G. Fraedrich, F. Kronenberg, The fate of patients with intermittent claudication in the 21st century revisited-results from the CAVASIC Study, Sci. Rep. 8 (2017), https://doi.org/10.1038/srep45833.

[4] M.M. McDermott, L. Ferrucci, M. Gonzalez-Freire, K. Kosmac, C. Leeuwenburgh, C. A. Peterson, S. Saini, R. Sufit, Skeletal muscle pathology in peripheral artery disease a brief review, Arterioscler. Thromb. Vasc. Biol. 40 (2020) 2577–2585, https://doi.org/10.1161/ATVBAHA.120.313831.

[5] G. Saenz-Pipaon, P. San Martín, N. Planell, A. Maillo, S. Ravassa, A. Vilas-Zornoza, E. Martinez-Aguilar, J.A. Rodriguez, D. Alameda, D. Lara-Astiaso, F. Prosper, J. A. Paramo, J. Orbe, D. Gomez-Cabrero, C. Roncal, Functional and transcriptomic analysis of extracellular vesicles identifies calprotectin as a new prognostic marker in peripheral arterial disease (PAD), J. Extracell. Vesicles 9 (2020), 1729646, https://doi.org/10.1080/20013078.2020.1729646.

[6] G. Saenz-Pipaon, S. Ravassa, K.L. Larsen, E. Martinez-Aguilar, J. Orbe, J. A. Rodriguez, L. Fernandez-Alonso, A. Gonzalez, J.L. Martín-Ventura, J.A. Paramo, J.S. Lindholt, C. Roncal, Lipocalin-2 and calprotectin potential prognosis biomarkers in peripheral arterial disease, Eur. J. Vasc. Endovasc. Surg. 63 (2022) 648–656, https://doi.org/10.1016/j.ejvs.2022.01.012.

[7] S. Chakraborty, S. Kaur, S. Guha, S.K. Batra, The multifaceted roles of neutrophil gelatinase associated lipocalin (NGAL) in inflammation and cancer, Biochim. Biophys. Acta Rev. Canc (2012), https://doi.org/10.1016/j.bbcan.2012.03.008.

[8] C.E. Fernandez-García, R. Roldan-Montero, C. Tarin, D. Martinez-Lopez, C. Pastor-Vargas, L.M. Blanco-Colio, J.L. Martín-Ventura, Lipocalin-2, a potential therapeutic target in advanced atherosclerosis, Atherosclerosis 278 (2018) 321–322, https://doi.org/10.1016/j.atherosclerosis.2018.07.036.

[9] J. Amersfoort, F.H. Schaftenaar, H. Douna, P.J. van Santbrink, M.J. Kröner, G.H. M. van Puijvelde, P.H.A. Quax, J. Kuiper, I. Bot, Lipocalin-2 Contributes to Experimental Atherosclerosis in a Stage-dependent Manner, Atherosclerosis, 2018, https://doi.org/10.1016/j.atherosclerosis.2018.06.015.

[10] A.L. Hemdahl, A. Gabrielsen, C. Zhu, P. Eriksson, U. Hedin, J. Kastrup, P. Thorén, G.K. Hansson, Expression of neutrophil gelatinase-associated lipocalin in atherosclerosis and myocardial infarction, Arterioscler. Thromb. Vasc. Biol. (2006), https://doi.org/10.1161/01.ATV.0000193567.88685.f4.

[11] B.C. Te Boekhorst, S.M. Bovens, W.E. Hellings, P.H. Van Der Kraak, K.W. Van De Kolk, A. Vink, F.L. Moll, M.F. Van Oosterhout, J.P. De Vries, P.A. Doevendans, M. J. Goumans, D.P. De Kleijn, C.J. Van Echteld, G. Pasterkamp, J.P. Sluijter, Molecular MRI of murine atherosclerotic plaque targeting NGAL: a protein associated with unstable human plaque characteristics, Cardiovasc. Res. (2011), https://doi.org/10.1093/cvr/cvq340.

[12] T. Varga, R. Mounier, A. Horvath, S. Cuvellier, F. Dumont, S. Poliska, H. Ardjoune, G. Juban, L. Nagy, B. Chazaud, Highly dynamic transcriptional signature of distinct macrophage subsets during sterile inflammation, resolution, and tissue repair, J. Immunol. 196 (2016) 4771–4782, https://doi.org/10.4049/jimmunol.1502490.

[13] I.A. Rebalka, C.M.F. Monaco, N.E. Varah, T. Berger, D.M. D'souza, S. Zhou, T. W. Mak, T.J. Hawke, Loss of the adipokine lipocalin-2 impairs satellite cell activation and skeletal muscle regeneration, Am. J. Physiol. Cell Physiol. (2018), https://doi.org/10.1152/ajpcell.00195.2017.

[14] D. Ye, K. Yang, S. Zang, Z. Lin, H.T. Chau, Y. Wang, J. Zhang, J. Shi, A. Xu, S. Lin, Y. Wang, Lipocalin-2 mediates non-alcoholic steatohepatitis by promoting neutrophil-macrophage crosstalk via the induction of CXCR2, J. Hepatol. 65 (2016) 988–997, https://doi.org/10.1016/j.jhep.2016.05.041.

[15] C.F. Bentzinger, Y.X. Wang, N.A. Dumont, M.A. Rudnicki, Cellular dynamics in the muscle satellite cell niche, EMBO Rep. 14 (2013) 1062–1072, https://doi.org/10.1038/EMBOR.2013.182.

[16] T. Berger, A. Togawa, G.S. Duncan, A.J. Elia, A. You-Ten, A. Wakeham, H.E. H. Fong, C.C. Cheung, T.W. Mak, Lipocalin 2-deficient mice exhibit increased sensitivity to Escherichia coli infection but not to ischemia-reperfusion injury, Proc. Natl. Acad. Sci. U.S.A. 103 (2006) 1834–1839, https://doi.org/10.1073/PNAS.0510847103.

[17] V. Gomez-Rodriguez, J. Orbe, E. Martinez-Aguilar, J.A.A. Rodriguez, L. Fernandez-Alonso, J. Serneels, M. Bobadilla, A. Perez-Ruiz, M. Collantes, M. Mazzone, J.A. A. Paramo, C. Roncal, Functional MMP-10 is required for efficient tissue repair after experimental hind limb ischemia, Faseb. J. 29 (2015) 960–972, fj.14-259689 [pii]10.1096/fj.14-259689.

[18] A.D. Chaudhuri, S.V. Yelamanchili, H.S. Fox, Combined fluorescent in situ hybridization for detection of microRNAs and immunofluorescent labeling for cell-type markers, Front. Cell. Neurosci. (2013), https://doi.org/10.3389/fncel.2013.00160.

[19] S.M.J. Welten, A.J.N.M. Bastiaansen, R.C.M. De Jong, M.R. De Vries, E.A.B. Peters, M.C. Boonstra, S.P. Sheikh, N. La Monica, E.R. Kandimalla, P.H.A. Quax, A. Yaël Nossent, Inhibition of 14q32 MicroRNAs miR-329, miR-487b, miR-494, and miR-495 increases neovascularization and blood flow recovery after ischemia, Circ. Res. 115 (2014) 696–708, https://doi.org/10.1161/CIRCRESAHA.114.304747.

[20] D. Costa, E. Principi, E. Lazzarini, F. Descalzi, R. Cancedda, P. Castagnola, S. Tavella, LCN2 overexpression in bone enhances the hematopoietic compartment via modulation of the bone marrow microenvironment, J. Cell. Physiol. 232 (2017) 3077–3087, https://doi.org/10.1002/jcp.25755.

[21] L. Guglani, R. Gopal, J. Rangel-Moreno, B.F. Junecko, Y. Lin, T. Berger, T.W. Mak, J.F. Alcorn, T.D. Randall, T.A. Reinhart, Y.R. Chan, S.A. Khader, Lipocalin 2

regulates inflammation during pulmonary mycobacterial infections, PLoS One 7 (2012), e50052, https://doi.org/10.1371/journal.pone.0050052.
[22] Y. Deng, D. Chen, F. Gao, H. Lv, G. Zhang, X. Sun, L. Liu, D. Mo, N. Ma, L. Song, X. Huo, T. Yan, J. Zhang, Z. Miao, Exosomes derived from microRNA-138-5p-overexpressing bone marrow-derived mesenchymal stem cells confer neuroprotection to astrocytes following ischemic stroke via inhibition of LCN2, J. Biol. Eng. 13 (2019), https://doi.org/10.1186/s13036-019-0193-0.
[23] A.F. Gombart, S.H. Kwok, K.L. Anderson, Y. Yamaguchi, B.E. Torbett, H.P. Koeffler, Regulation of neutrophil and eosinophil secondary granule gene expression by transcription factors C/EBPε and PU.1, Blood 101 (2003) 3265–3273, https://doi.org/10.1182/blood-2002-04-1039.
[24] J.M. Warszawska, R. Gawish, O. Sharif, S. Sigel, B. Doninger, K. Lakovits, I. Mesteri, M. Nairz, L. Boon, A. Spiel, V. Fuhrmann, B. Strobl, M. Müller, P. Schenk, G. Weiss, S. Knapp, Lipocalin 2 deactivates macrophages and worsens pneumococcal pneumonia outcomes, J. Clin. Invest. 123 (2013) 3363–3372, https://doi.org/10.1172/JCI67911.
[25] H. Guo, D. Jin, X. Chen, Lipocalin 2 is a regulator of macrophage polarization and NF-κB/STAT3 pathway activation, Mol. Endocrinol. 28 (2014) 1616–1628, https://doi.org/10.1210/me.2014-1092.
[26] W. Eilenberg, S. Stojkovic, A. Piechota-Polanczyk, C. Kaun, S. Rauscher, M. Gröger, M. Klinger, J. Wojta, C. Neumayer, I. Huk, S. Demyanets, Neutrophil gelatinase-associated lipocalin (NGAL) is associated with symptomatic carotid atherosclerosis and drives pro-inflammatory state *in vitro*, Eur. J. Vasc. Endovasc. Surg. 51 (2016) 623–631, https://doi.org/10.1016/j.ejvs.2016.01.009.
[27] R. Oberoi, E.P. Bogalle, L.A. Matthes, H. Schuett, A.K. Koch, K. Grote, B. Schieffer, J. Schuett, M. Luchtefeld, Lipocalin (LCN) 2 mediates pro-atherosclerotic processes and is elevated in patients with coronary artery disease, PLoS One 10 (2015), e0137924, https://doi.org/10.1371/journal.pone.0137924.
[28] L. Cheng, H. Xing, X. Mao, L. Li, X. Li, Q. Li, Lipocalin-2 promotes M1 macrophages polarization in a mouse cardiac ischaemia-reperfusion injury model, Scand. J. Immunol. 81 (2015) 31–38, https://doi.org/10.1111/sji.12245.
[29] C. Tarín, C.E. Fernandez-Garcia, E. Burillo, C. Pastor-Vargas, P. Llamas-Granda, B. Castejón, P. Ramos-Mozo, M.M. Torres-Fonseca, T. Berger, T.W. Mak, J. Egido, L.M. Blanco-Colio, J.L. Martín-Ventura, Lipocalin-2 deficiency or blockade protects against aortic abdominal aneurysm development in mice, Cardiovasc. Res. 111 (2016) 262–273, https://doi.org/10.1093/CVR/CVW112.
[30] E. Martínez-Martínez, M. Buonafine, I. Boukhalfa, J. Ibarrola, A. Fernández-Celis, P. Kolkhof, P. Rossignol, N. Girerd, P. Mulder, N. López-Andrés, A. Ouvrard-Pascaud, F. Jaisser, Aldosterone target NGAL (Neutrophil gelatinase-associated lipocalin) is involved in cardiac remodeling after myocardial infarction through NFκB pathway, Hypertension 70 (2017) 1148–1156, https://doi.org/10.1161/HYPERTENSIONAHA.117.09791.
[31] P.G. Kamble, M.J. Pereira, K. Almby, J.W. Eriksson, Estrogen interacts with glucocorticoids in the regulation of lipocalin 2 expression in human adipose tissue. Reciprocal roles of estrogen receptor α and β in insulin resistance? Mol. Cell. Endocrinol. 490 (2019) 28–36, https://doi.org/10.1016/J.MCE.2019.04.002.
[32] K. Chella Krishnan, S. Sabir, M. Shum, Y. Meng, R. Acín-Pérez, J.M. Lang, R. R. Floyd, L. Vergnes, M.M. Seldin, B.K. Fuqua, D.W. Jayasekera, S.K. Nand, D. C. Anum, C. Pan, L. Stiles, M. Péterfy, K. Reue, M. Liesa, A.J. Lusis, Sex-specific metabolic functions of adipose Lipocalin-2, Mol. Metabol. 30 (2019) 30–47, https://doi.org/10.1016/j.molmet.2019.09.009.
[33] A. Tarjus, E. Martínez-Martínez, C. Amador, C. Latouche, S. El Moghrabi, T. Berger, T.W. Mak, R. Fay, N. Farman, P. Rossignol, F. Zannad, N. López-Andrés, F. Jaisser, Neutrophil gelatinase-associated lipocalin, a novel mineralocorticoid biotarget, mediates vascular profibrotic effects of mineralocorticoids, Hypertension 66 (2015) 158–166, https://doi.org/10.1161/HYPERTENSIONAHA.115.05431.
[34] B. Bonnard, E. Martínez-Martínez, A. Fernández-Celis, M. Pieronne-Deperrois, Q. T. Do, I. Ramos, P. Rossignol, F. Zannad, P. Mulder, A. Ouvrard-Pascaud, N. López-Andrés, F. Jaisser, Antifibrotic effect of novel neutrophil gelatinase-associated lipocalin inhibitors in cardiac and renal disease models, Sci. Rep. 11 (2021) 1–11, https://doi.org/10.1038/s41598-021-82279-0.
[35] J. Yang, B. McNeish, C. Butterfield, M.A. Moses, Lipocalin 2 is a novel regulator of angiogenesis in human breast cancer, FASEB J. Off. Publ. Fed. Am. Soc. Exp. Biol. 27 (2013) 45–50, https://doi.org/10.1096/fj.12-211730.
[36] L. Wu, Y. Du, J. Lok, E.H. Lo, C. Xing, Lipocalin-2 enhances angiogenesis in rat brain endothelial cells via reactive oxygen species and iron-dependent mechanisms, J. Neurochem. 132 (2015) 622–628, https://doi.org/10.1111/jnc.13023.
[37] Z. Tong, A.B. Kunnumakkara, H. Wang, Y. Matsuo, P. Diagaradjane, K. B. Harikumar, V. Ramachandran, B. Sung, A. Chakraborty, R.S. Bresalier, C. Logsdon, B.B. Aggarwal, S. Krishnan, S. Guha, Neutrophil gelatinase-associated lipocalin: a novel suppressor of invasion and angiogenesis in pancreatic cancer, Cancer Res. 68 (2008) 6100–6108, https://doi.org/10.1158/0008-5472.CAN-08-0540.
[38] D. Pérez-Cremades, H.S. Cheng, M.W. Feinberg, Noncoding RNAs in critical limb ischemia, Arterioscler. Thromb. Vasc. Biol. 40 (2019) 523–533, https://doi.org/10.1161/ATVBAHA.119.312860.
[39] W. Zhou, W. Zhou, Q. Zeng, J. Xiong, MicroRNA-138 inhibits hypoxia-induced proliferation of endothelial progenitor cells via inhibition of HIF-1α-mediated MAPK and AKT signaling, Exp. Ther. Med. 13 (2017) 1017–1024, https://doi.org/10.3892/etm.2017.4091.
[40] A. Sen, S. Ren, C. Lerchenmüller, J. Sun, N. Weiss, P. Most, K. Peppel, MicroRNA-138 regulates hypoxia-induced endothelial cell dysfunction by targeting S100A1, PLoS One 8 (2013), https://doi.org/10.1371/journal.pone.0078684.
[41] S. Sun, C. Wang, J. Weng, MicroRNA-138-5p drives the progression of heart failure via inhibiting sirtuin 1 signaling, Mol. Med. Rep. 23 (2021), https://doi.org/10.3892/mmr.2021.11915.
[42] A. Bogucka-Kocka, D.P. Zalewski, K.P. Ruszel, A. Stępniewski, D. Gałkowski, J. Bogucki, Ł. Komsta, P. Kołodziej, T. Zubilewicz, M. Feldo, J. Kocki, Dysregulation of MicroRNA regulatory network in lower extremities arterial disease, Front. Genet. (2019), https://doi.org/10.3389/fgene.2019.01200.
[43] D.P. Zalewski, K.P. Ruszel, A. Stępniewski, D. Gałkowski, M. Feldo, J. Kocki, A. Bogucka-Kocka, Application of OpenArray RT-qPCR for identification of microRNA expression signatures of lower extremity artery disease, J. Appl. Genet. 63 (2022) 497–512, https://doi.org/10.1007/S13353-022-00692-1.
[44] H. Xiong, T. Luo, W. He, D. Xi, H. Lu, M. Li, J. Liu, Z. Guo, Up-regulation of miR-138 inhibits hypoxia-induced cardiomyocyte apoptosis via down-regulating lipocalin-2 expression, Exp. Biol. Med. 241 (2016) 25–30, https://doi.org/10.1177/1535370215591831.
[45] W.R. Hiatt, E.J. Armstrong, C.J. Larson, E.P. Brass, Pathogenesis of the limb manifestations and exercise limitations in peripheral artery disease, Circ. Res. (2015), https://doi.org/10.1161/CIRCRESAHA.116.303566.
[46] M.E. Padgett, T.J. McCord, J.M. McClung, C.D. Kontos, Methods for acute and subacute murine hindlimb ischemia, 2016, J. Vis. Exp. (2016), 54166, https://doi.org/10.3791/54166.
[47] L. Terlecki-Zaniewicz, I. Lämmermann, J. Latreille, M.R. Bobbili, V. Pils, M. Schosserer, R. Weinmüllner, H. Dellago, S. Skalicky, D. Pum, J.C.H. Almaraz, M. Scheideler, F. Morizot, M. Hackl, F. Gruber, J. Grillari, Small extracellular vesicles and their miRNA cargo are anti-apoptotic members of the senescence-associated secretory phenotype, Aging (N Y) 10 (2018) 1103–1132, https://doi.org/10.18632/AGING.101452.